Study on the Formation Mechanism of Fish-Scale Defects during Flow Forming of Copper Alloy Tubes with Large Thickness-to-Diameter Ratio

Qinxiang Xia[1], *Jie* Zhao[1], *Gangfeng* Xiao[1*], *Delin* Tang[2] , and *Huachun* Cui[2]

[1]School of Mechanical and Automotive Engineering, South China University of Technology, Guangzhou 510641, China
[2]Co., Ltd of Yantai Wanlong Vacuum Metallurgy, Yantai 264000, China

Abstract. Flow forming is one of the most effective methods for producing tube-shaped parts. However, fish-scale defects occur easily during the flow forming of copper alloy tubes with large thickness-to-diameter ratio, which significantly affects the surface quality and performance of the spun tubes. The reason for the formation of fish-scale defects and the microstructural characteristics in the defective regions were investigated experimentally, the deformation behavior and strain distribution of materials were revealed through finite element simulation. The results show that fish-scale defects are a folding phenomenon caused by local instability during forming; deformation concentrates on the outer surface due to the large thickness-to-diameter ratio of the tubular blank and the low hardening index of the copper alloy; the plastic deformation ability of the material on the outer surface decreases with the increasing of deformation degree, which leads to local flow instability and results in the formation of fish-scale defects.

Keywords: Flow Forming; Large Thickness-to-Diameter Ratio; Copper Alloy; Fish-Scale Defect

1 Introduction

The copper alloy tubes used in subsea pipelines are typical large-thickness-to-diameter ratio components, with outer diameters exceeding 300 mm and a thickness-to-diameter ratio greater than 0.1. Due to prolonged exposure to seabed pressure, seawater impact, and environmental factors, these tubes require excellent corrosion resistance, wear resistance, and high strength[1,2].

Currently, large-thickness-to-diameter ratio tubes are typically produced through processes such as "casting-bulging-piercing-extrusion" or "casting-extrusion composite forming"[3]. However, these methods have some drawbacks, including lengthy process flows and issues such as coarse grain size and porosity in the final product. Flow spinning, a thinning metal spinning process, provides an alternative to address these limitations. In this process, the tube blank is mounted on a rotating mandrel, and a roller applies axial pressure, inducing plastic deformation at the contact point. This results in a reduction of wall thickness and an increase in tube length. Flow spinning efficiently produces high-performance, dense-structured tubes, offering an effective solution for forming large diameter tubes with superior properties[4]. However, during the flow spinning of copper alloy tubes with a large thickness-to-diameter ratio, defects such as fish-scale often appear on the tube surface. These defects necessitate subsequent surface cutting treatments, limiting further improvements in production efficiency and material performance.*

Previous studies have shown that fish-scale defects are related to material folding caused by the roller pressing[5,6]. Rajan[7] pointed out through flow spinning tests on high-strength SAE4130 steel that excessively small roller roundness radius and feed ratios can lead to uneven deformation and increased residual stresses, making the occurrence of fish-scale defects more likely. Bhatt[8] indicated in flow spinning tests on 6061 aluminum alloy tubes that excessive spindle speeds and low thinning rates result in uneven material flow and increased strain hardening, which further promotes local deformation instability and the formation of fish-scale defects.

However, it is challenging to fully capture the stress-strain distribution, material flow, and other forming characteristics during the process through experimental tests alone. This makes it difficult to explore the formation mechanism of fish-scale defects in depth. As the diameter and thickness of the tube blank increase, the mechanisms behind defect formation become more complex, and the research cost and difficulty of experimental testing increase significantly. This paper aims to combine experimental analysis with finite element simulations to examine the deformation behavior of large-thickness-to-diameter ratio copper alloy tubes during flow spinning, investigate the formation mechanism of fish-scale defects, and provide a theoretical basis for addressing these defects.

*Corresponding author: xiaogf@scut.edu.cn

© The Authors, published by EDP Sciences. This is an open access article distributed under the terms of the Creative Commons Attribution License 4.0 (https://creativecommons.org/licenses/by/4.0/).

2 Experiments and Simulation

2.1 Flow Spinning Forming Experiment

This study focuses on copper alloy tubing for subsea pipelines, specifically BFe10-1-1. The tube blank has an outer diameter of D_0=385mm and a thickness of t_0=39.5mm, yielding a thickness-to-diameter ratio of 0.1. The blank undergoes vacuum casting, followed by multiple passes of free forging and turning. The flow spinning process is used to reduce the thickness to t_f=19.7mm. To improve forming efficiency, a three-roller reverse flow spinning process (as shown in Figure 1) is employed, with the tail end of the tube blank in contact with a thrust ring and rotating synchronously with the spindle[9]. The rollers feature a double-cone structure, with a attack angle of α_p=25°and a roundness radius of r_p=R18. The rollers are evenly distributed every 120° around the circumference and are synchronized in the forming process.

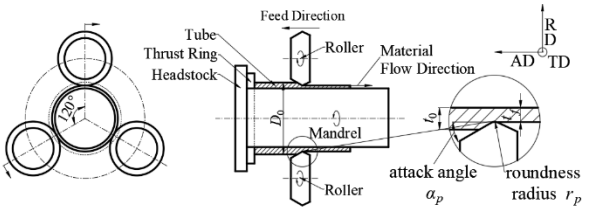

Fig. 1. Three-roller reverse flow spinning process

The thinning rate ψ and feed ratio f are critical parameters influencing the stability and deformation during the spinning process. For small-diameter tubes, the optimal thinning rate ψ_n is between 30% and 45%, and the feed ratio f can range from 0.2 to 1.0 mm/r. When the feed ratio is fixed, the spindle speed n has minimal impact on the experimental results, as long as it matches the equipment's performance. In the flow spinning process, the axial spinning force F_x is commonly used to measure the stability of forming. The formula for calculating F_x is given by Equation 1[10].

$$F_x = \frac{kt_0}{t_0 - t_f}\left[\ln\left(\frac{t_0}{t_f}\right)\left(\sqrt{6}\alpha_p + m_1\cos\alpha_p + m_2\right) + 2\left(1-\cos\alpha_p\right)\right] \quad (1)$$

Which m_1 is the coefficient of friction between the roller and the workpiece, and m_2 is the coefficient of friction between the workpiece and the mandrel.

Since an increase in Fx is detrimental to stable forming, and Fx increases with the tube blank thickness when the thinning rate remains constant, a smaller thinning rate is selected, and the forming is performed in multiple passes. The process parameters are shown in Table 2.

Table 2. Process parameter values

Pass	t_0/mm	ψ_n/%	n/(r/min)	f/(mm/r)
1	39.5	21.5	35	0.875
2	31	22.6	26	0.65
3	24	17.3	26	0.65

The experiment is conducted by a 500T heavy-duty spinning machine. At the end of the first pass, the tube surface is smooth (as shown in Figure 2a). Following the second pass, small scales appear on the smooth surface . After the third pass, the tube surface shows fish-scales overall (as shown in Figure 2b).

a）Pass1

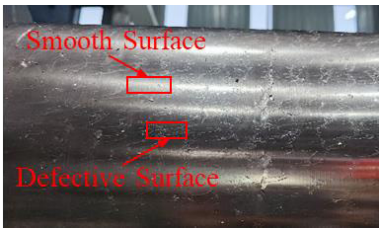

b）Pass3

Fig. 2. Outer surface of copper alloy tubing

2.2 Finite Element Modeling

Finite element simulation provides a comprehensive representation of stress-strain distribution, material flow, and other characteristics during the forming process, thereby aiding in the analysis of the formation mechanism of fish-scale defects. In this study, a finite element model for flow spinning was established by ABAQUS software, as shown in Figure 3. The roller profile dimensions, workpiece diameter, and process parameters were set to align with those used in the experiments (as listed in Table 1). To balance computational efficiency and accuracy, the tube blank length was set to l=300mm. Furthermore, to improve model convergence and computational efficiency, the thrust ring and spindle were omitted, and the tail end of the tube blank was fixed, with the roller performing both circumferential and axial feed motions during the simulation[11].

The model adopts a penalty contact model. In the forming experiments, the copper alloy blank have smooth surfaces, with coolant sprayed on the outer surface and no lubrication applied to the inner surface, thus friction coefficients were set to m_1=0.08 between the roller and workpiece, and m_2=0.15 between the blank and mandrel. To prevent excessive mesh deformation, ALE (Arbitrary Lagrangian-Eulerian) mesh adaptation is applied.

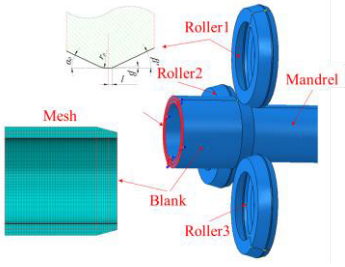

Fig. 3. Flow spinning finite element model

3 Results and Discussion

3.1 Metallographic Analysis

At the end of the third pass forming, samples were taken from both the smooth area between fish-scales and the defect area with fish-scales (as shown in Figure 2b). These samples were sectioned, ground progressively with abrasive papers (from 240 to 3000 grit), and polished using a 0.5 μm alumina (Al_2O_3) suspension. Subsequently, the polished specimens were chemically etched with an aqueous solution containing ferric chloride and hydrochloric acid for 1 minute to reveal the microstructure. Metallographic observations were then conducted using a DMI 5000M microscope at magnifications of 200× and 500×.

Figure 4 shows the smooth area, where the material exhibits a layered structure with parallel metal flow lines along the axial direction. These lines are more densely distributed near the outer surface, indicating stable forming and concentrated deformation at the outer surface.

Figure 5 shows the defect area, where the metal flow lines are disordered. A gap is observed 60 μm from the outer surface, penetrating the layered structure. The metal flow lines on either side of the gap are discontinuous. Compared with the parallel metal flow lines observed in the smooth region, a vortex-like pattern appears in the right side of the defective region, which is the initiation site of the defect. This suggests local flow instability, with fish-scale caused by material folding, resulting in the characteristic fish-scale patterns.

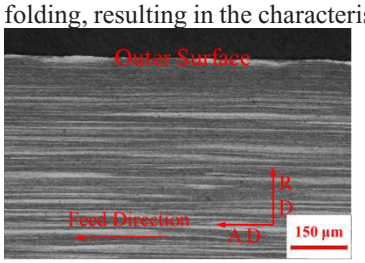

Fig. 4. Metallography of the smooth area

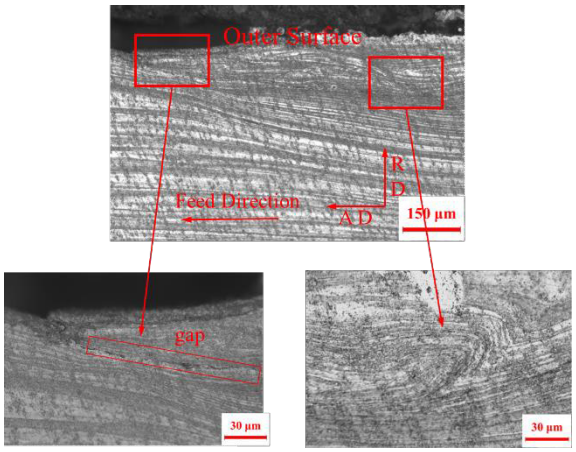

Fig. 5. Metallography of the defect area

3.2 Material Flow Analysis

Taking the first pass as an example for the forming process analysis, the variation of the spinning force over time is shown in Figure 6. Based on the force trend, the flow spinning process can be divided into the start and stable stages. During the start stage, the roller's effect on the workpiece gradually increases, and material begins to accumulate in front of the roller. In the steady stage, material flow reaches equilibrium, and the stress-strain in the forming zone stabilizes.

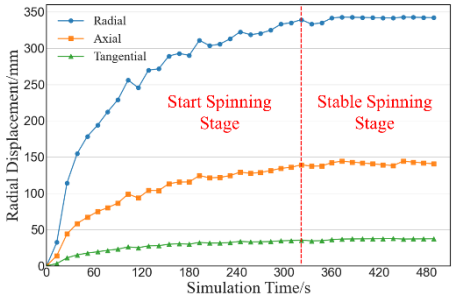

Fig. 6. Spinning force variation curve

Points were selected from the outer surface, middle position, and inner surface of the tube blank to track their radial displacements during deformation. The resulting is shown in Figure 7. At both the outer surface and middle position, the radial displacement first increases and then decreases during deformation. This indicates that, unlike in the flow spinning of small-diameter tubes, in large-thickness-to-diameter ratio copper alloy tubes, the material in the undeformed zone bulges upward before flowing into the deformed zone, rather than directly flowing into the formed zone at an angle less than or equal to the roller's forming angle (as shown in Figure 8) [12].

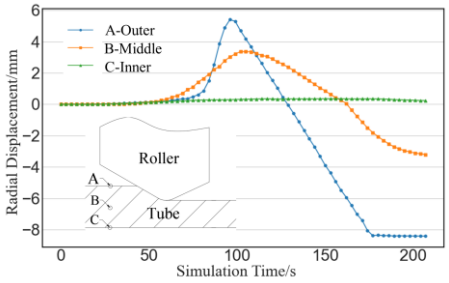

Fig. 7. Forming time - radial displacement curve

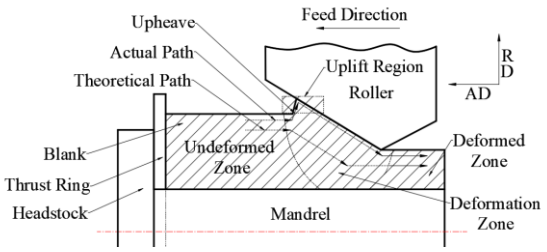

Fig. 8. Material flow schematic

3.3 Strain Analysis

Figure 9 shows the three-dimensional plastic strain contour maps during the stable spinning stage of each pass (directions as shown in Figure 1). The primary deformation consists of radial compression and axial elongation. In the first pass, deformation is concentrated at the outer surface, with strain exhibiting a gradient distribution along the thickness direction. Significant

tangential deformation occurs at the outer surface of the tube blank. In the second pass, large axial and radial deformations occur at the inner surface, and the strain difference between the inner and outer surfaces gradually decreases. A more uniform strain distribution is achieved in the third pass.

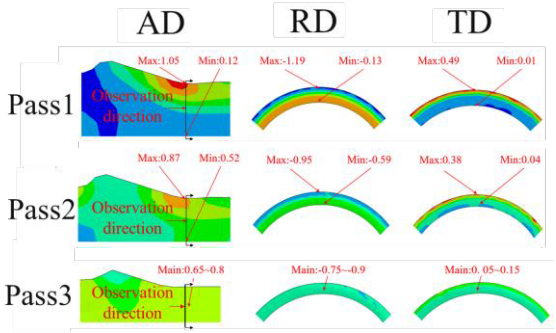

Fig. 9. Three-dimensional plastic strain contour map

Equivalent plastic strain (PEEQ) is used to quantify the overall degree of material deformation. Unlike plastic strain (PE), which measures the final deformation state, PEEQ is the time integral of the equivalent plastic strain rate (as shown in Equation 2). It records the cumulative strain and provides a better description of material deformation under the complex loading conditions of spinning. A larger PEEQ value indicates more complete material deformation and a higher degree of work hardening[13].

$$\mathrm{PEEQ}(t)=\int_0^t\sqrt{\frac{2}{3}\dot{\varepsilon}^p\dot{\varepsilon}^p}\,dt \tag{2}$$

The units are numbered based on their radial distance from the outer surface of the material. The trend of equivalent plastic strain at different radial positions of the material at the end of each pass is shown in Figure 10. The results indicate that in the first pass, deformation is concentrated near the outer surface, with significant deformation occurring at the outer surface, while the material near the inner surface experiences minimal deformation. In the second pass, the tube blank deforms more uniformly, with the PEEQ at the inner surface increasing to 4.9, and the ratio of inner to outer surface PEEQ rising to 14.8%. In the third pass, plastic deformation is concentrated near the inner surface, while the PEEQ value at the outer surface remains largely unchanged. This suggests that after the first two passes, the material at the outer surface has undergone substantial work hardening, resulting in reduced flowability. In the third pass, almost no plastic deformation occurs at the outer surface, further confirming that the material has become significantly hardened and less able to deform.

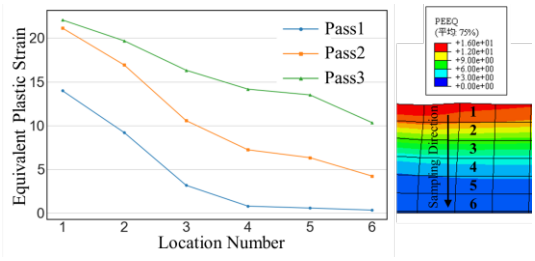

Fig. 10. Equivalent plastic strain distribution

3.4 Analysis of Fish-Scale Defects

In flow spinning, the roller contacts the outer surface material, initiating deformation at the outer surface. As the outer surface material gradually hardens, the deformation shifts toward the inner surface. Finite element simulations show that in the flow spinning of large-thickness-to-diameter ratio copper alloy tubes, strain exhibits a significant radial gradient distribution (as shown in Figure 9). After the first two passes, the material at the outer surface undergoes considerable work hardening, reducing its flowability. This results in folding during the third pass due to local deformation instability.

Compared to the inner material, the outer surface material experiences significant upward bulging and tangential deformation during the process (as shown in Figures 8 and 9). The complex deformation path is a key factor contributing to the increased hardening of the outer surface material. In flow spinning, the S/L ratio is commonly used to measure the material flow behavior during forming, where S represents the tangential contact length between the roller and the workpiece, and L represents the axial contact length. A larger S/L ratio indicates a greater axial flow tendency of the material, which improves workpiece dimensional accuracy and surface quality. In contrast, a smaller S/L ratio leads to a greater tangential flow tendency, increasing the instability of the forming process. The formulas for calculating S and L are as follows[5]:

$$S=R_R\beta \tag{3}$$

$$L\approx\frac{t_0-t_f}{\tan\alpha_p}+f \tag{4}$$

$$\beta=\cos^{-1}\left(\frac{a^2+c^2-b^2}{2ac}\right) \tag{5}$$

Where R_R is the radius of the roller, and a, b, and c are the geometrical lengths related to the mold, as shown in Figure 11.

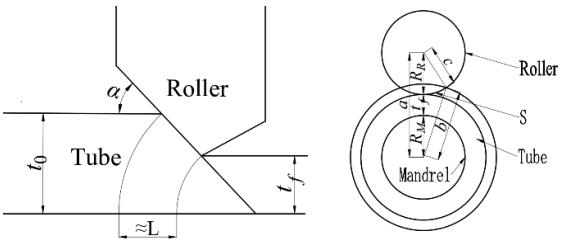

Fig. 11. S/L calculation schematic diagram

In the flow spinning, as the tube diameter increases, S slightly increases. However, with an increase in tube thickness, the thinning amount also increases, leading to a significant rise in L, and consequently, a substantial decrease in the S/L ratio. In the three passes, the S/L ratios are 0.50, 0.52, and 0.83, respectively, indicating a tendency for the material to flow tangentially. The increase in tangential flow promotes tangential deformation at the outer surface, while restricting material flow along the axial direction, causing the outer surface material to bulge. This results in both tangential deformation and upward bulging of the material as it flows from the undeformed to the deformed zone,

accumulating more deformation and leading to significant work hardening. Additionally, the BFe10-1-1 alloy has a limited work hardening capacity, making it difficult for deformation to effectively transfer to the inner layers. As a result, deformation is concentrated at the outer surface, which is directly in contact with the roller, contributing to the formation of fish-scale defects[14].

In summary, the fish-scale defects are attributed to the structural characteristics of the large-thickness-to-diameter ratio tube and the limited hardening capacity of copper alloys. The outer surface material accumulates more deformation during the forming process. As the number of forming passes increases, significant work hardening occurs at the outer surface, reducing flowability and ultimately leading to local deformation instability and folding, which results in the formation of fish-scale patterns on the outer surface.

4 Conclusion

This study, based on forming experiments and finite element simulations, investigates the mechanism of fish-scale defects in the flow spinning of large-thickness-to-diameter ratio copper alloy tubes, analyzing their formation and underlying causes.

(1) Flow spinning experiments on large-thickness-to-diameter ratio copper alloy tubes revealed that fish-scale defects primarily occur during the third pass. Metallographic analysis showed that these defects arise from local deformation instability, resulting in fish-scale-like folding patterns.

(2) A finite element model for the flow spinning of large-thickness-to-diameter ratio copper alloy tubes was developed using ABAQUS software. The simulations demonstrated a clear gradient distribution of strain along the radial direction. Compared to the inner surface, the outer surface material undergoes significant tangential deformation and upward bulging as it flows from the undeformed to the deformed zone. This complex deformation path leads to increased deformation accumulation and significant work hardening, which, combined with reduced flowability, makes the outer surface material more susceptible to fish-scale defects.

(3) Analysis based on the S/L ratio formula revealed that the structural characteristics of large-thickness-to-diameter ratio tubes promote tangential flow of the material, causing tangential deformation and material bulging. This behavior is a key factor contributing to the significant hardening of the outer surface and the formation of fish-scale defects. Furthermore, the limited work hardening capacity of copper alloys exacerbates the development of these defects

Acknowledgments

This work was supported by the Key R&D Program of Shandong Province (023CXGC010403) and the Foundation of Basic and Applied Basic Research of Guangdong Province (2024A1515240047).

References

1. A. Cheng, N.Z. Chen, Int. J. Press. Ves. Pip. **199**, 104711 (2022)
2. Q. Liu, P. Li, B. Wu, Coatings **14**(7), 834 (2024)
3. L. Jia, Y. Li, T. Hui, Chin. J. Mech. Eng. 32, 1 (2019)
4. Y.T. Li, L. Jia, J.H. Fu, Patent: China ZL201310025737.4 (2013)
5. G. Xiao, Q. Xia, X. Cheng, et al., MATEC Web Conf. **21**, 03007 (2015)
6. Gur M, Tirosh J, J. Mater. Process. Technol. **66**, 195(1997)
7. B. Podder, P. Banerjee, K.R. Kumar, et al., Sādhan ā. **43**, 1 (2018)
8. K.M. Rajan, K. Narasimhan, Pract. Fail. Anal. **1**, 69 (2001)
9. R.J. Bhatt, H.K. Raval, Mater. Today Proc. **5**(2), 7230 (2018)
10. Q. Xia, Novel Spinning Forming Technology (Science Press, Beijing, 2017)
11. N. Kim, H. Kim, K. Jin, Int. J. Precis. Eng. Manuf. **14**, 259 (2013)
12. Q. Xia, J. Long, G. Xiao, et al., J. Mater. Process. Technol. **296**, 117197 (2021)
13. J.W. Park, Y.H. Kim, W.B. Bae, J. Mater. Process. Technol. **66**(1–3), 195 (1997)
14. W. Yuan, Y.F. Pan, Y.P. Yu, C. Li, G. Han, Z.Y. Zhou, Mater. Mech. Eng. **47**(12), 12 (2023)